

Detecting Mild Traumatic Brain Injury with MEG Scan

Data: One-vs-K-Sample Tests

—Supplementary Materials

Jian Zhang

School of Mathematics, Statistics and Actuarial Science

University of Kent, Canterbury, CT2 7NF, UK

j.zhang-79@kent.ac.uk

Gary Green

Innovision IP Ltd

Culham Innovation Centre

D5 Culham Science Centre

Abingdon

Oxfordshire OX14 3DB

and

Department of Psychology

University of York, York, YO10 5DD, UK

gary.green@york.ac.uk

The Supplementary Materials are organised as follows. In Section 1, we provide a list of brain areas of interest in terms of the Desikan-Killiany Atlas. In Section 2, we present the results of applying the FLR-HC and PAD-HC to the abnormal areas claimed by the FLR and PAD respectively. In Section 3, we demonstrate the abilities of the PAD-HC and the FLR-HC in capturing heterogeneity in controls and in separating the case from controls.

1 Brain areas of interest: the Desikan-Killiany Atlas

Index	Region Name
1	ctx-lh-bankssts
2	ctx-lh-caudalanteriorcingulate
3	ctx-lh-caudalmiddlefrontal
4	ctx-lh-cuneus
5	ctx-lh-entorhinal
6	ctx-lh-frontalpole
7	ctx-lh-fusiform
8	ctx-lh-inferiorparietal
9	ctx-lh-inferiortemporal
10	ctx-lh-insula
11	ctx-lh-isthmuscingulate
12	ctx-lh-lateraloccipital
13	ctx-lh-lateralorbitofrontal
14	ctx-lh-lingual
15	ctx-lh-medialorbitofrontal
16	ctx-lh-middletemporal
17	ctx-lh-paracentral
18	ctx-lh-parahippocampal
19	ctx-lh-parsopercularis
20	ctx-lh-parsorbitalis
21	ctx-lh-parstriangularis
22	ctx-lh-pericalcarine
23	ctx-lh-postcentral
24	ctx-lh-posteriorcingulate
25	ctx-lh-precentral
26	ctx-lh-precuneus
27	ctx-lh-rostralanteriorcingulate
28	ctx-lh-rostralmiddlefrontal
29	ctx-lh-superiorfrontal
30	ctx-lh-superiorparietal

31 ctx-lh-superiortemporal
32 ctx-lh-supramarginal
33 ctx-lh-temporalpole
34 ctx-lh-transversetemporal
35 ctx-rh-bankssts
36 ctx-rh-caudalanteriorcingulate
37 ctx-rh-caudalmiddlefrontal
38 ctx-rh-cuneus
39 ctx-rh-entorhinal
40 ctx-rh-frontalpole
41 ctx-rh-fusiform
42 ctx-rh-inferiorparietal
43 ctx-rh-inferiortemporal
44 ctx-rh-insula
45 ctx-rh-isthmuscingulate
46 ctx-rh-lateraloccipital
47 ctx-rh-lateralorbitofrontal
48 ctx-rh-lingual
49 ctx-rh-medialorbitofrontal
50 ctx-rh-middletemporal
51 ctx-rh-paracentral
52 ctx-rh-parahippocampal
53 ctx-rh-parsopercularis
54 ctx-rh-parsorbitalis
55 ctx-rh-parstriangularis
56 ctx-rh-pericalcarine
57 ctx-rh-postcentral
58 ctx-rh-posteriorcingulate
59 ctx-rh-precentral
60 ctx-rh-precuneus
61 ctx-rh-rostralanteriorcingulate
62 ctx-rh-rostralmiddlefrontal

63 ctx-rh-superiorfrontal
64 ctx-rh-superiorparietal
65 ctx-rh-superiortemporal
66 ctx-rh-supramarginal
67 ctx-rh-temporalpole
68 ctx-rh-transversetemporal

2 Results on hierarchical clustering

In the following, in addition to Figures 8 and 9 in the main text, we present the dendrograms for the abnormal areas claimed by the FLR and PAD in the delta- and gamma-band respectively. We select these areas, where the case-subject 55 is the last one to be merged into the dendrogram, as the FLR-HC and PAD-HC adjusted areas.

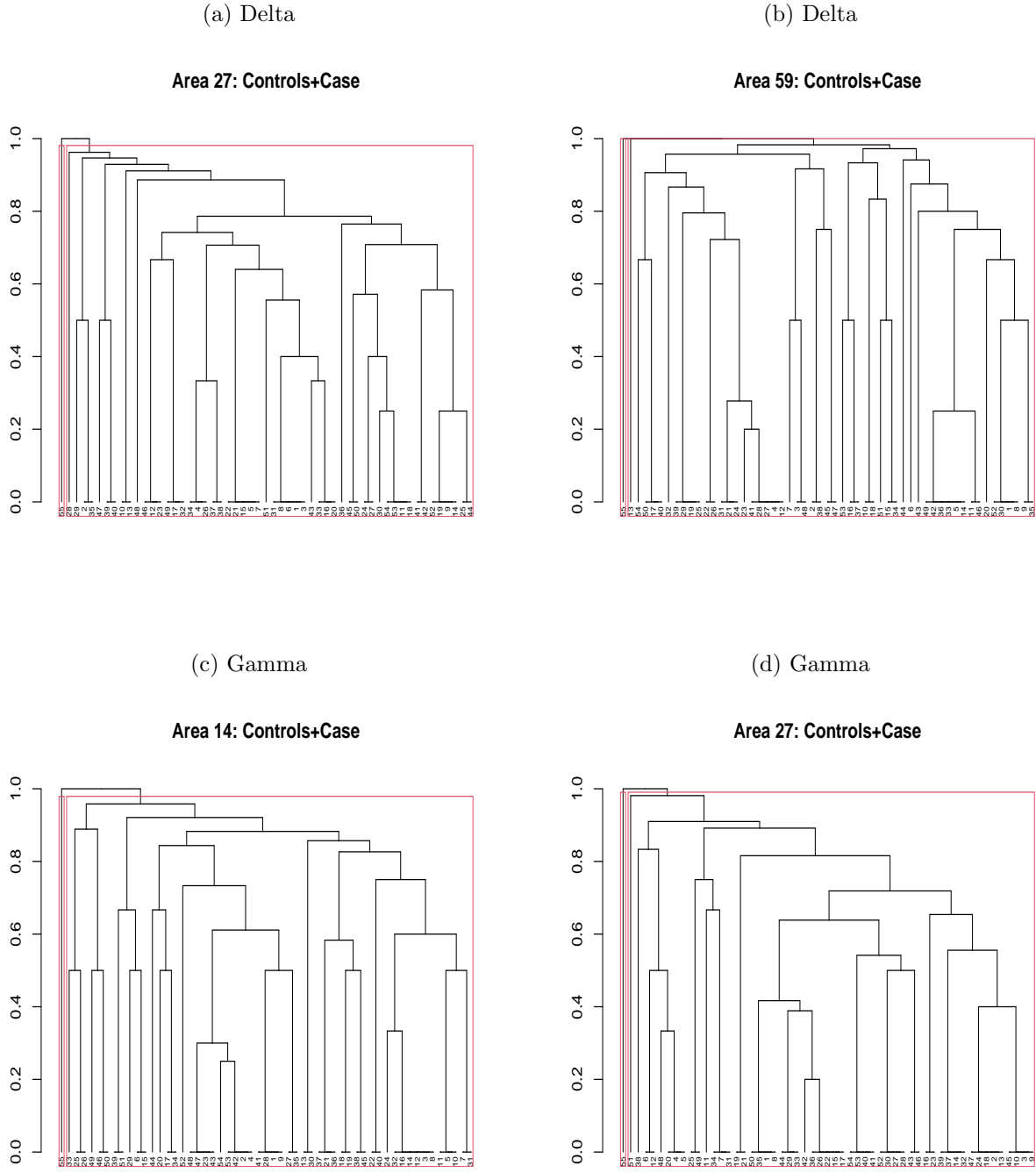


Figure 1: Examples of the FLR-HC dendrograms for the delta- and gamma- band data. Red boxes indicate the cluster borders if we partition 55 subjects into two clusters.

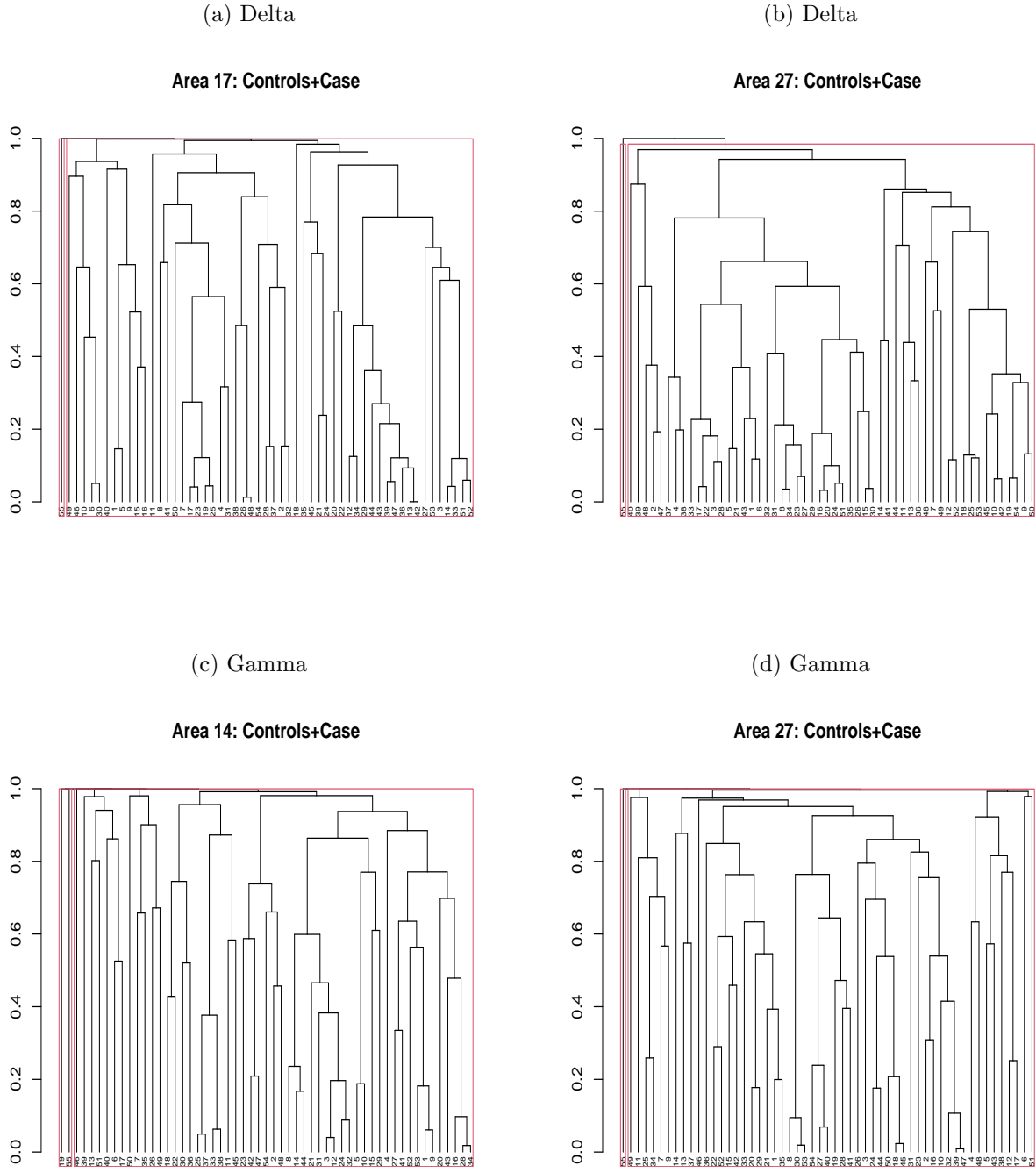


Figure 2: Examples of the PAD-HC dendrograms for the delta- and gamma- band data. Red boxes indicate the cluster borders if we partition 55 subjects into two clusters.

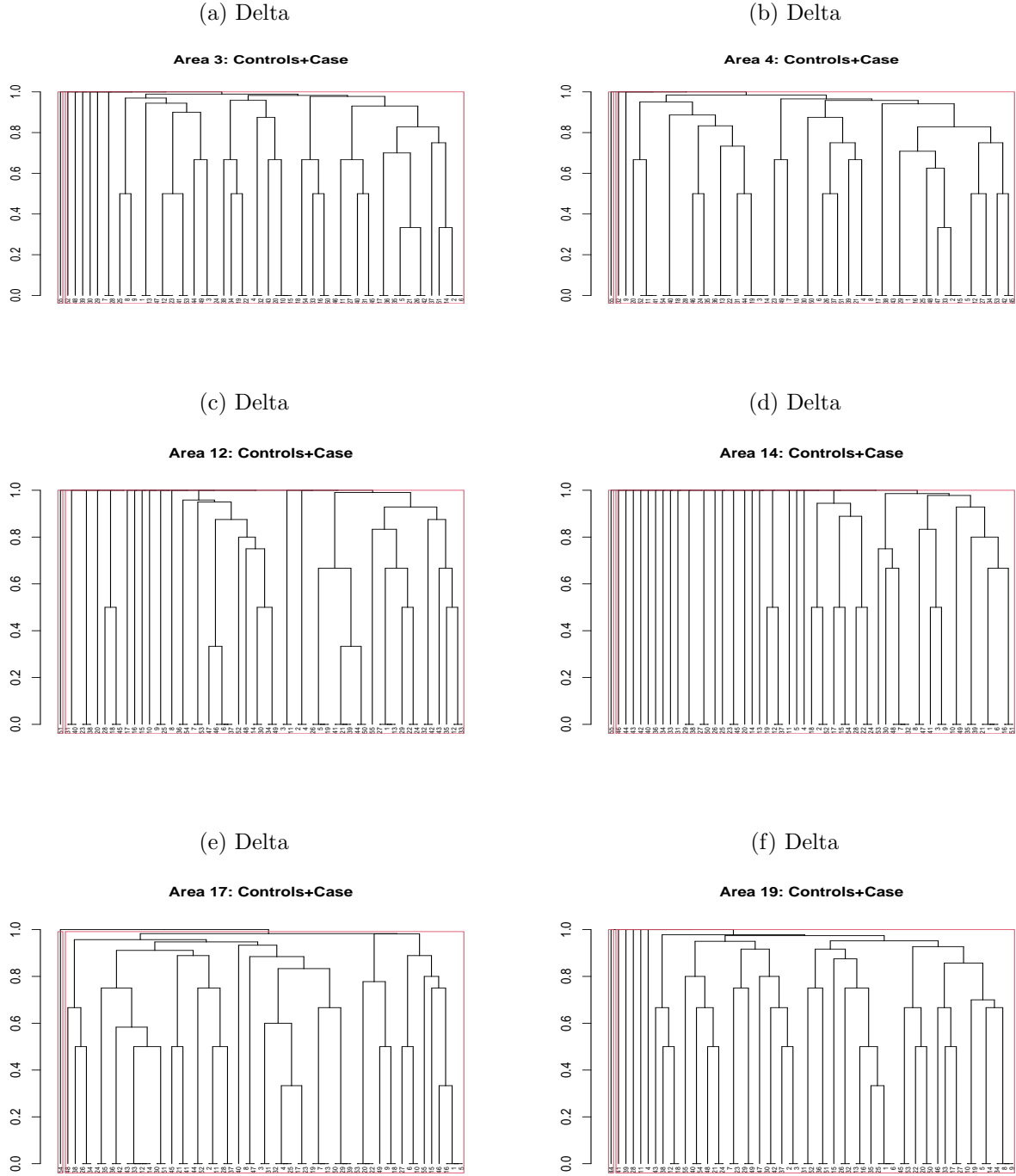


Figure 3: FLR-HC dendrograms for the areas identified as positive by the FLR in the delta band. Red boxes indicate the cluster borders if we partition 55 subjects into two clusters.

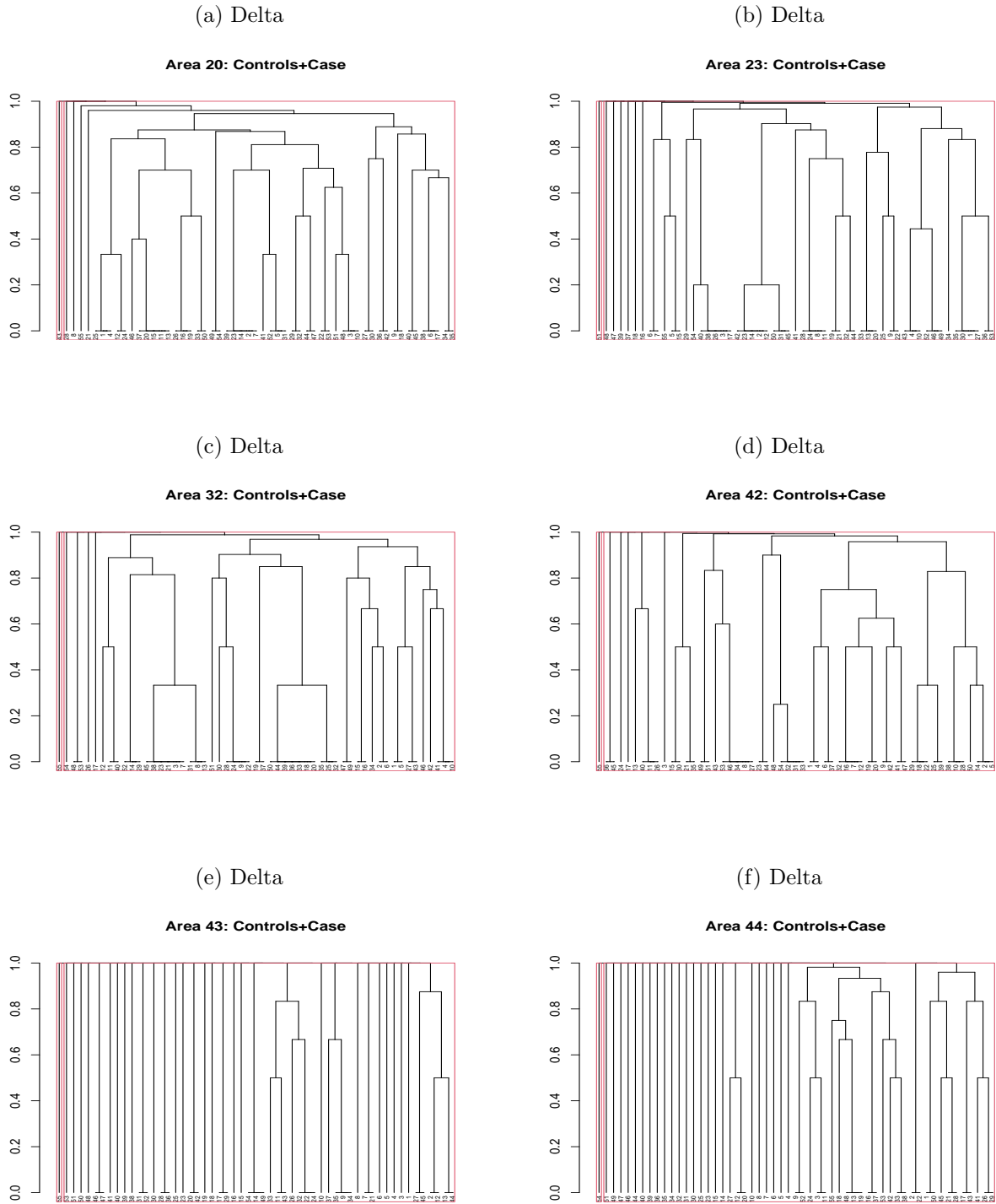


Figure 4: FLR-HC dendrograms for the areas identified as positive by the FLR in the delta band. Red boxes indicate the cluster borders if we partition 55 subjects into two clusters.

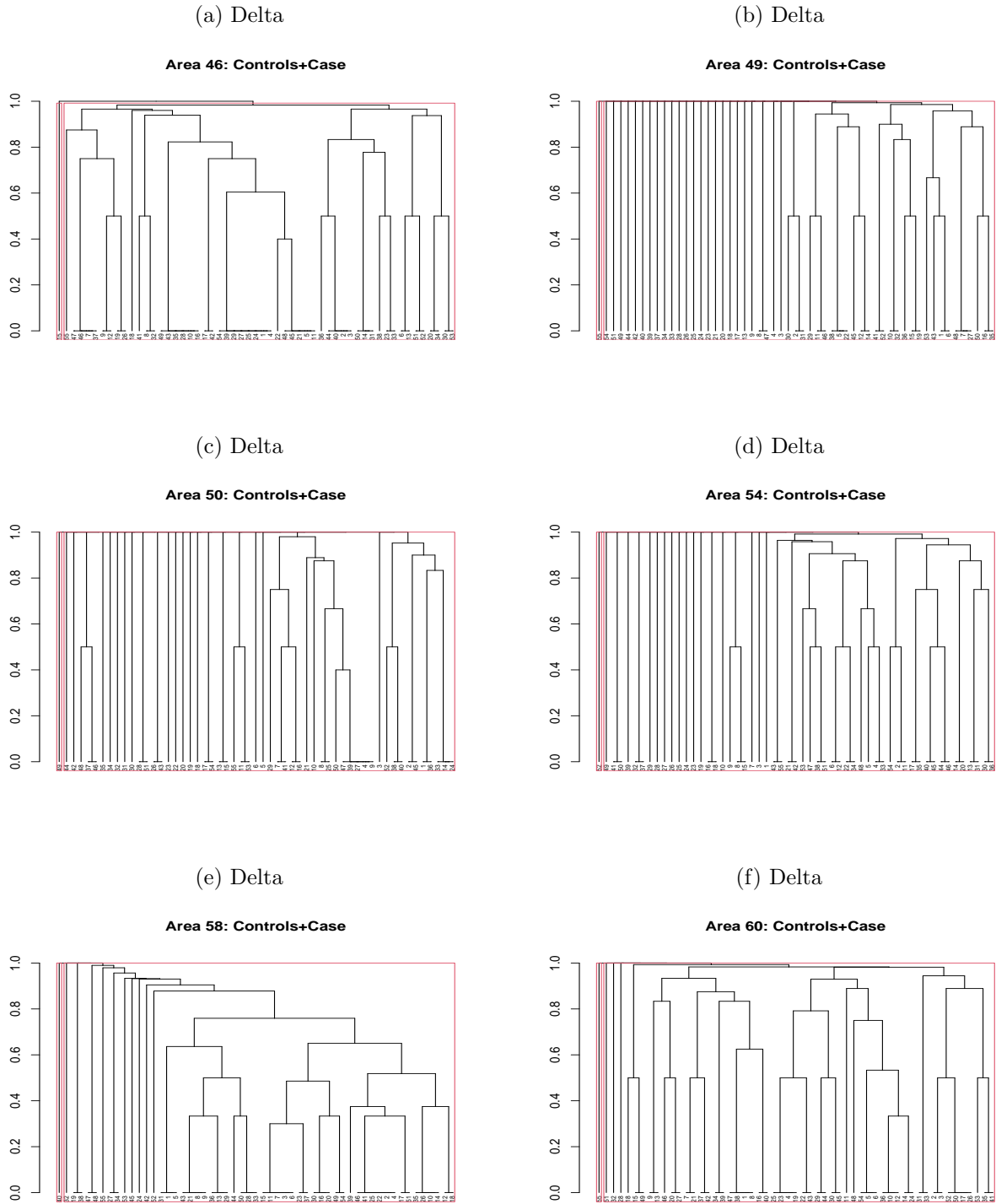


Figure 5: FLR-HC dendrograms for the areas identified as positive by the FLR in the delta band. Red boxes indicate the cluster borders if we partition 55 subjects into two clusters.

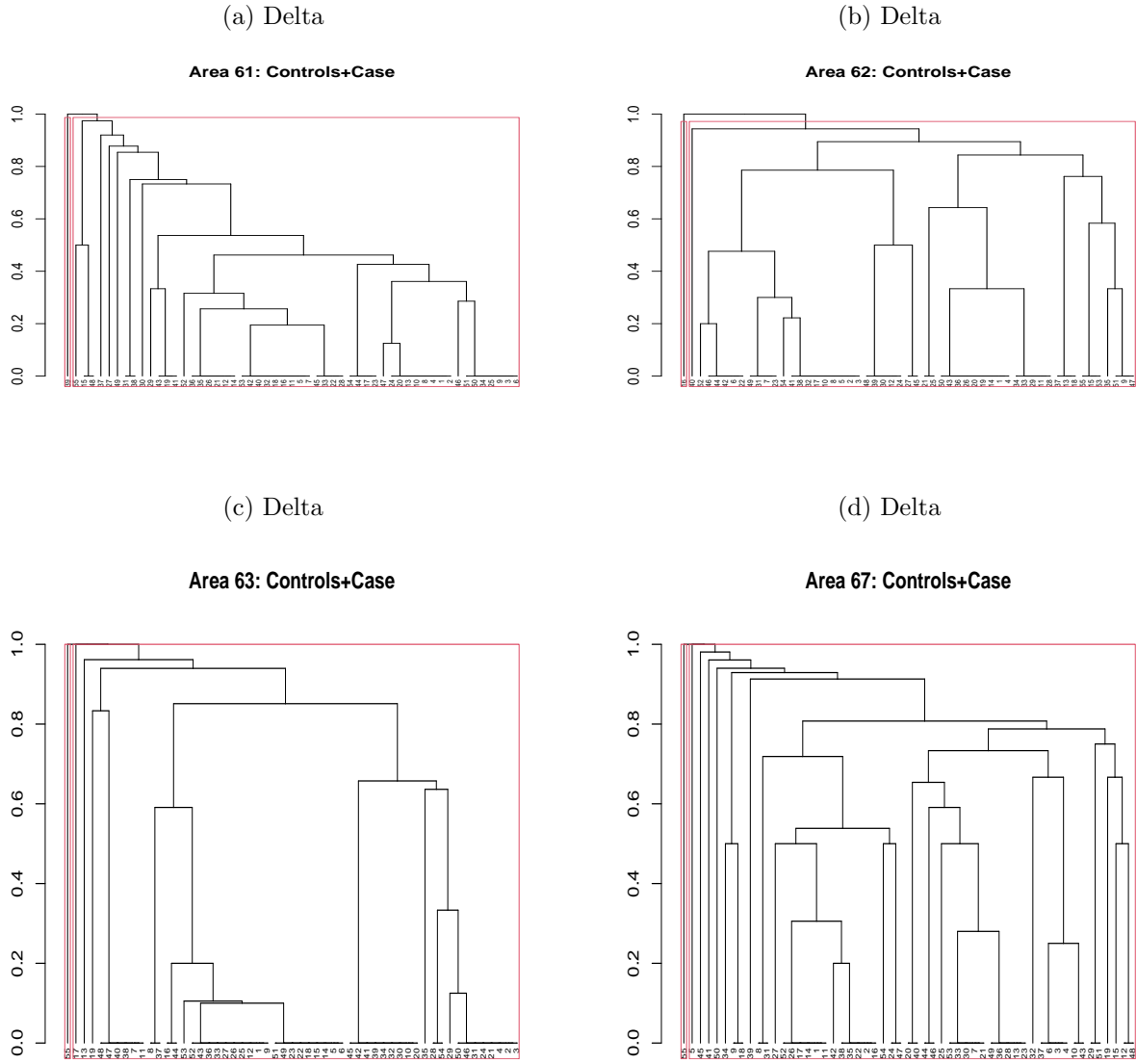


Figure 6: FLR-HC dendrograms for the areas identified as positive by the FLR in the delta band. Red boxes indicate the cluster borders if we partition 55 subjects into two clusters.

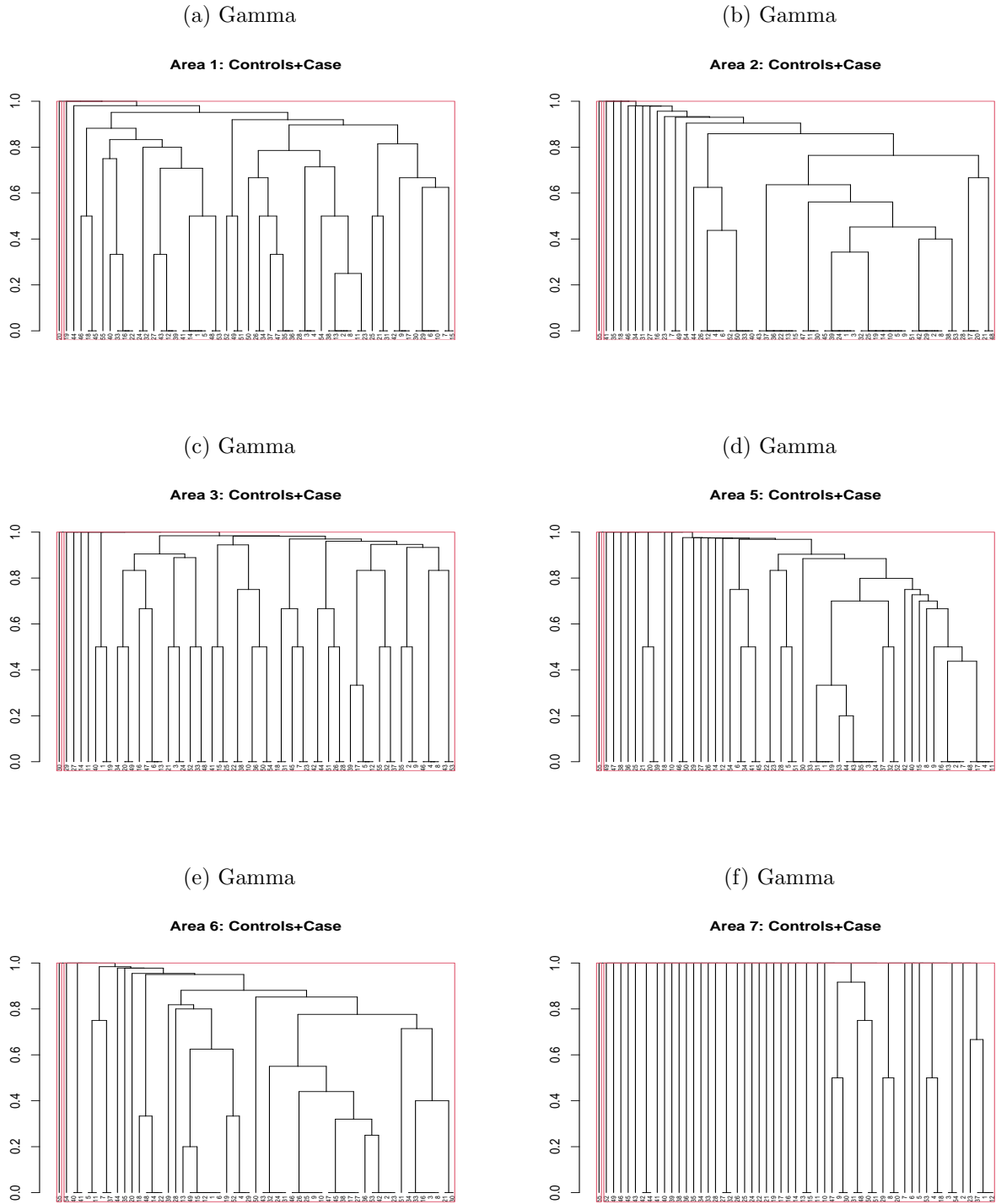


Figure 7: FLR-HC dendrograms for the areas identified as positive by the FLR in the gamma band. Red boxes indicate the cluster borders if we partition 55 subjects into two clusters.

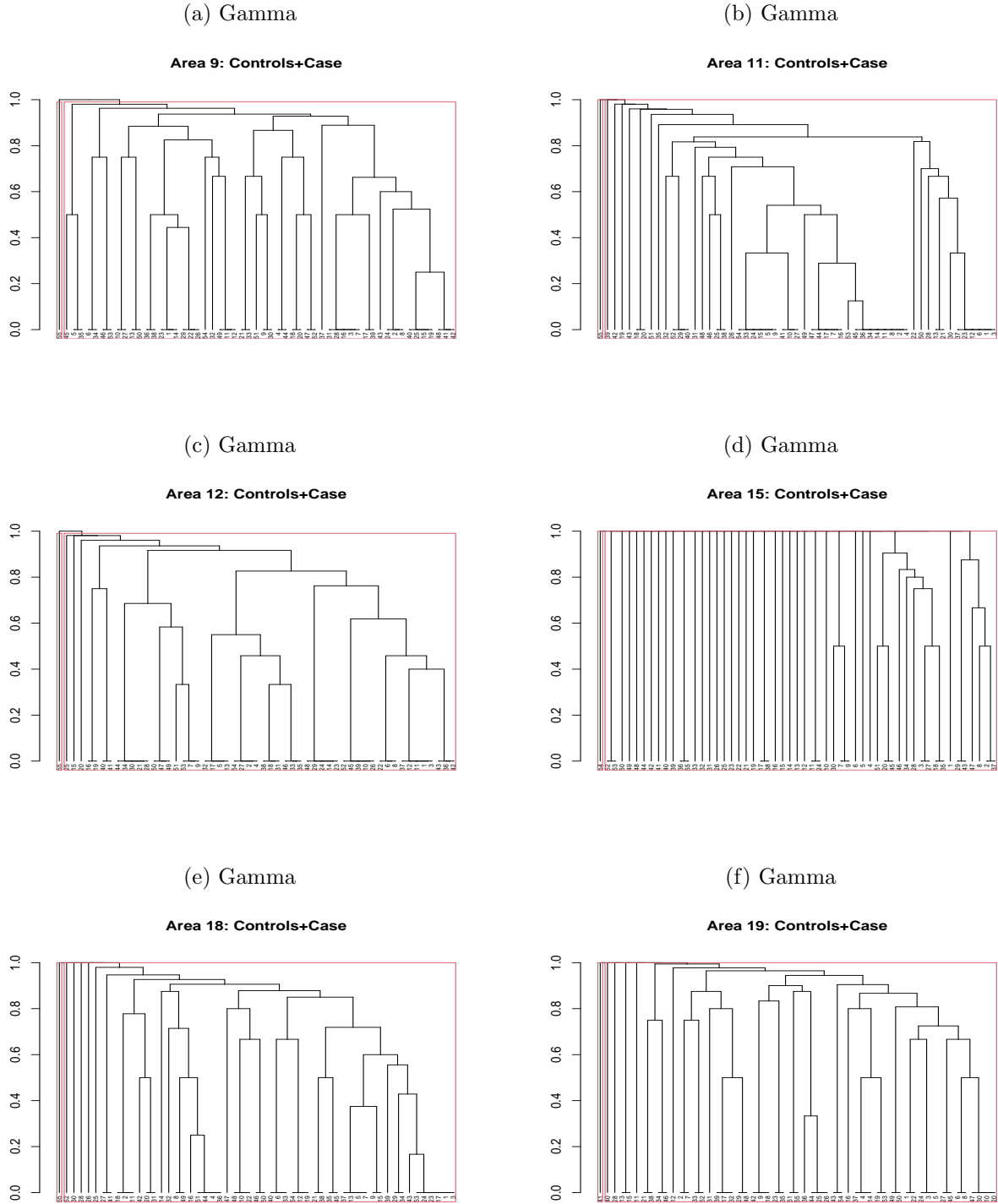


Figure 8: FLR-HC dendrograms for the areas identified as positive by the FLR in the gamma band. Red boxes indicate the cluster borders if we partition 55 subjects into two clusters.

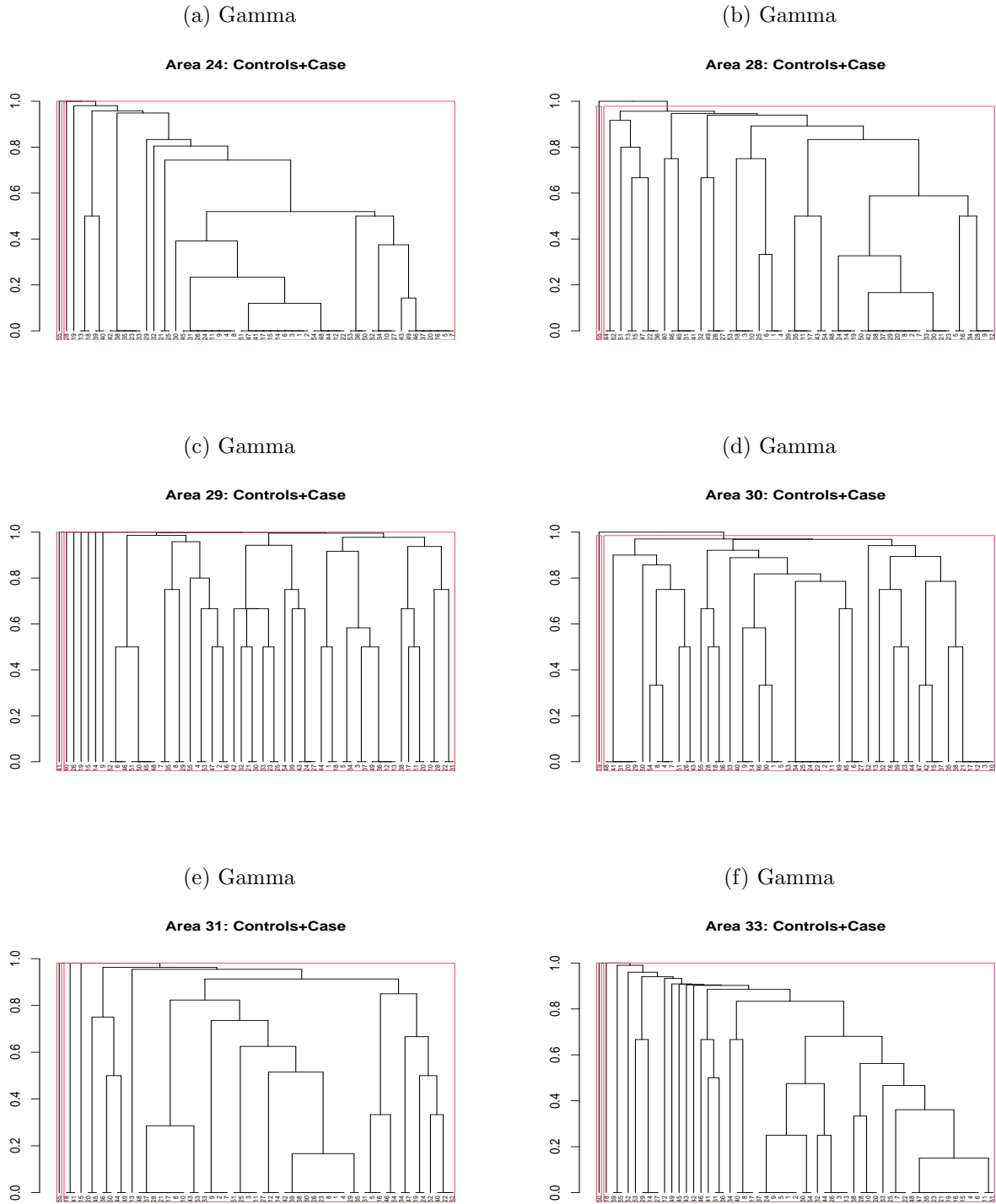


Figure 9: FLR-HC dendrograms for the areas identified as positive by the FLR in the gamma band. Red boxes indicate the cluster borders if we partition 55 subjects into two clusters.

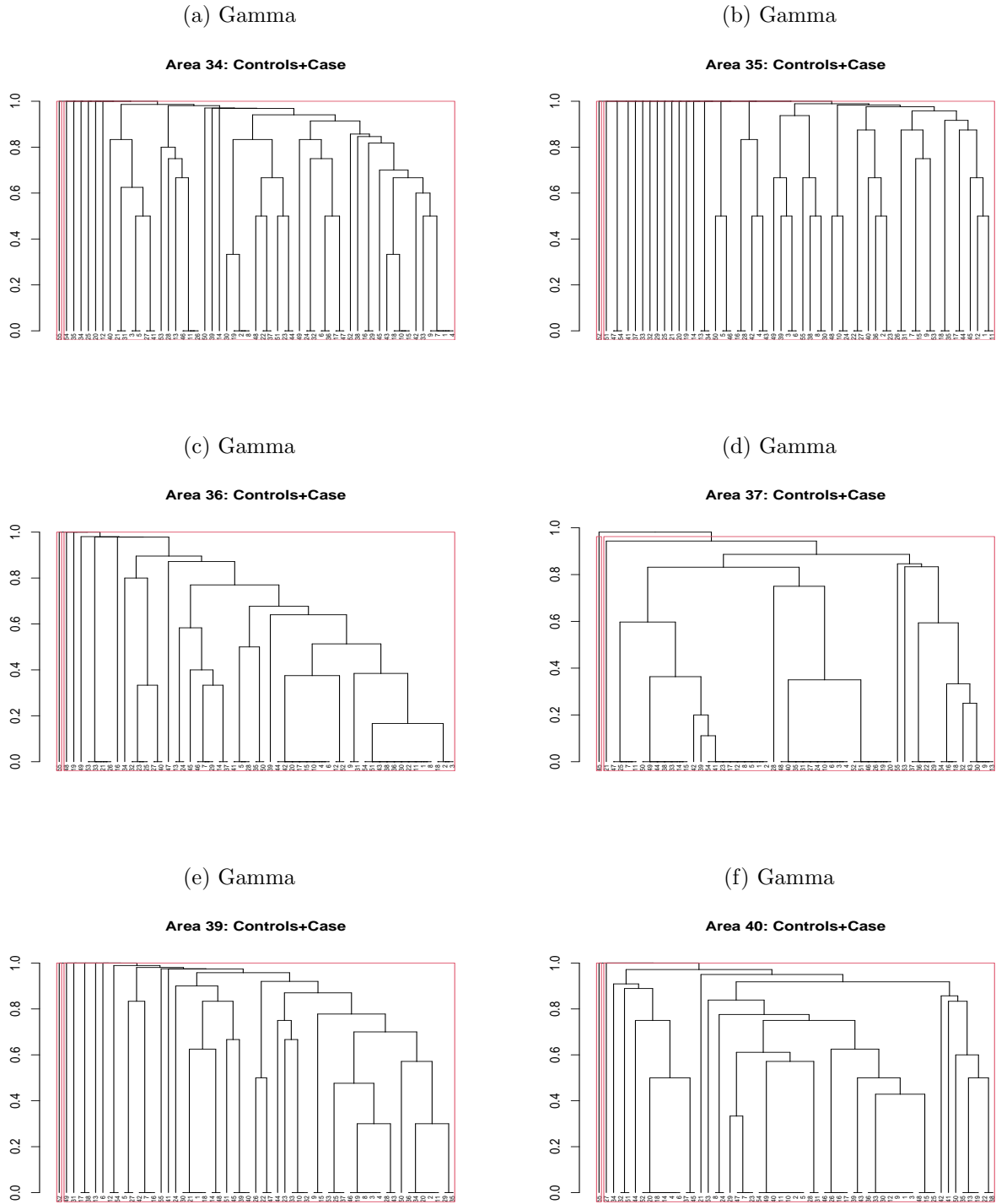


Figure 10: FLR-HC dendrograms for the areas identified as positive by the FLR in the gamma band. Red boxes indicate the cluster borders if we partition 55 subjects into two clusters.

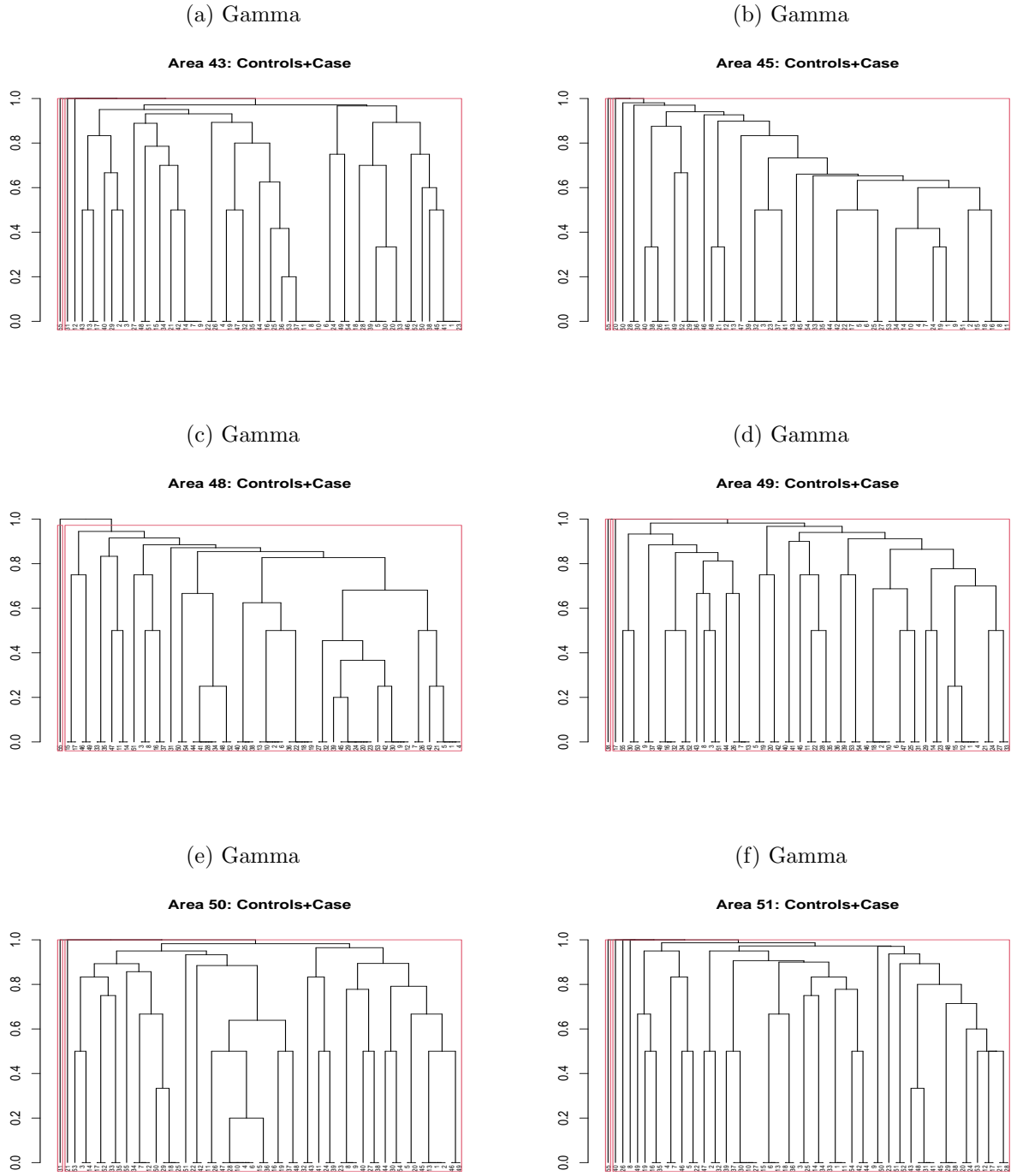


Figure 11: FLR-HC dendrograms for the areas identified as positive by the FLR in the gamma band. Red boxes indicate the cluster borders if we partition 55 subjects into two clusters.

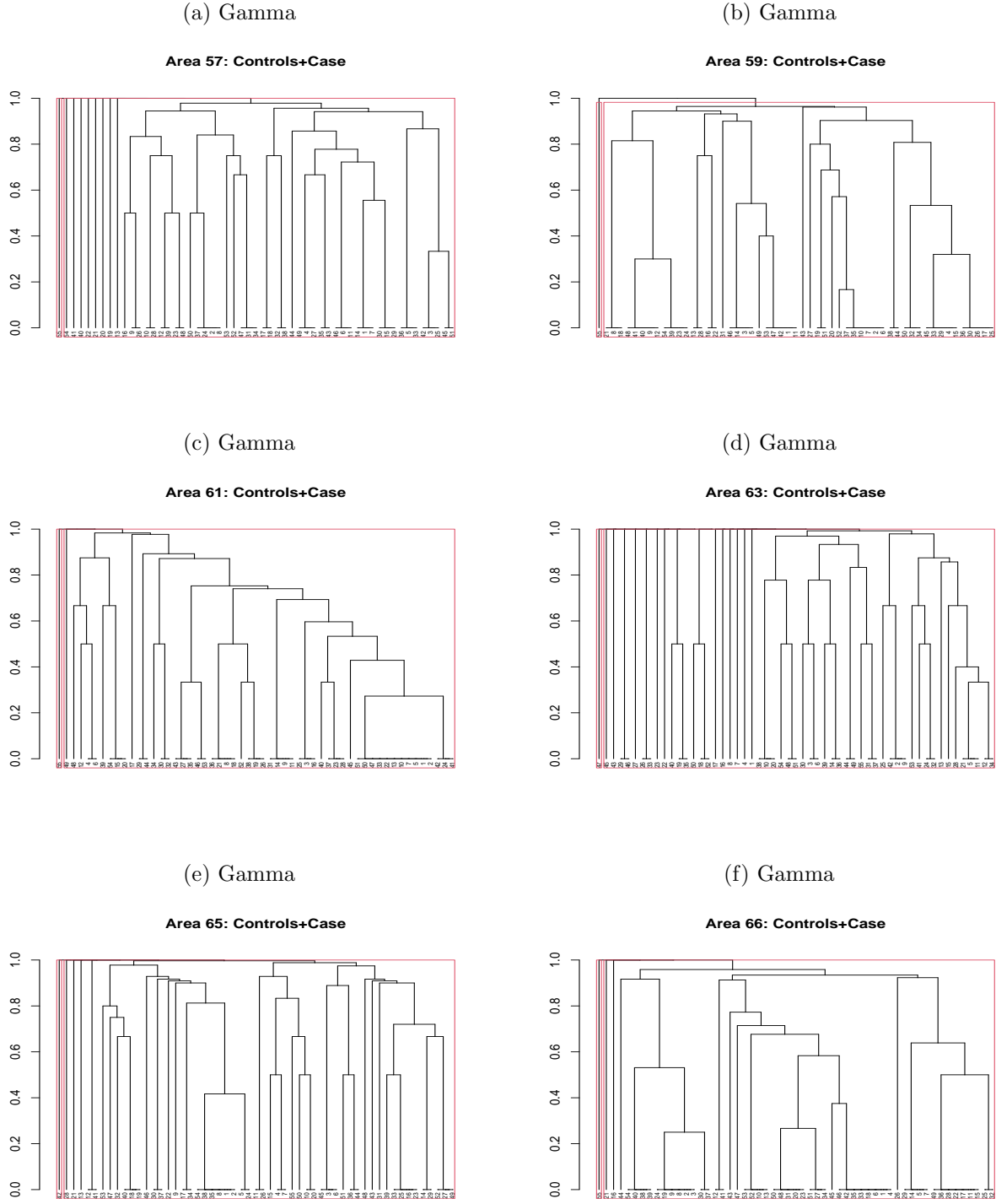


Figure 12: FLR-HC dendrograms for the areas identified as positive by the FLR in the gamma band. Red boxes indicate the cluster borders if we partition 55 subjects into two clusters.

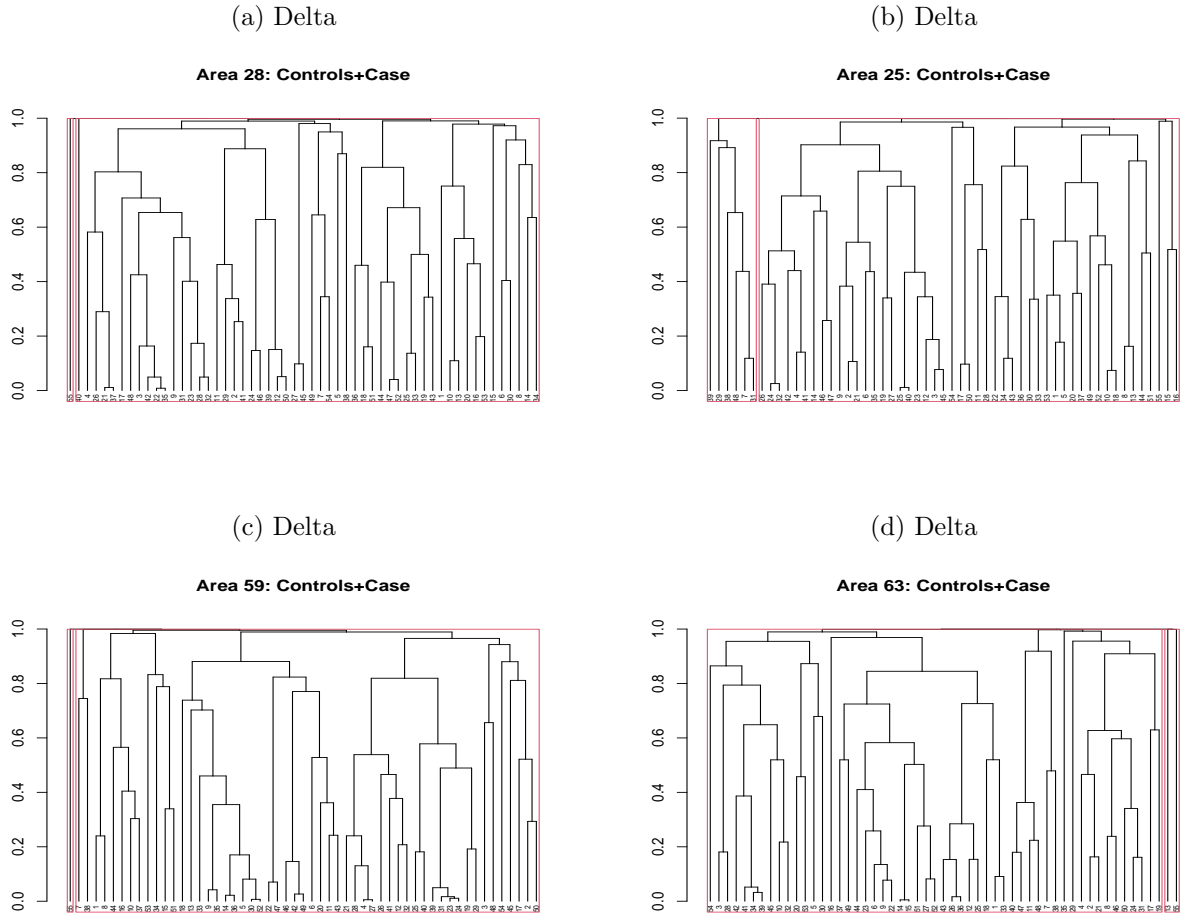


Figure 13: PAD-HC dendrograms in the delta band. Red boxes indicate the cluster borders if we partition 55 subjects into two clusters.

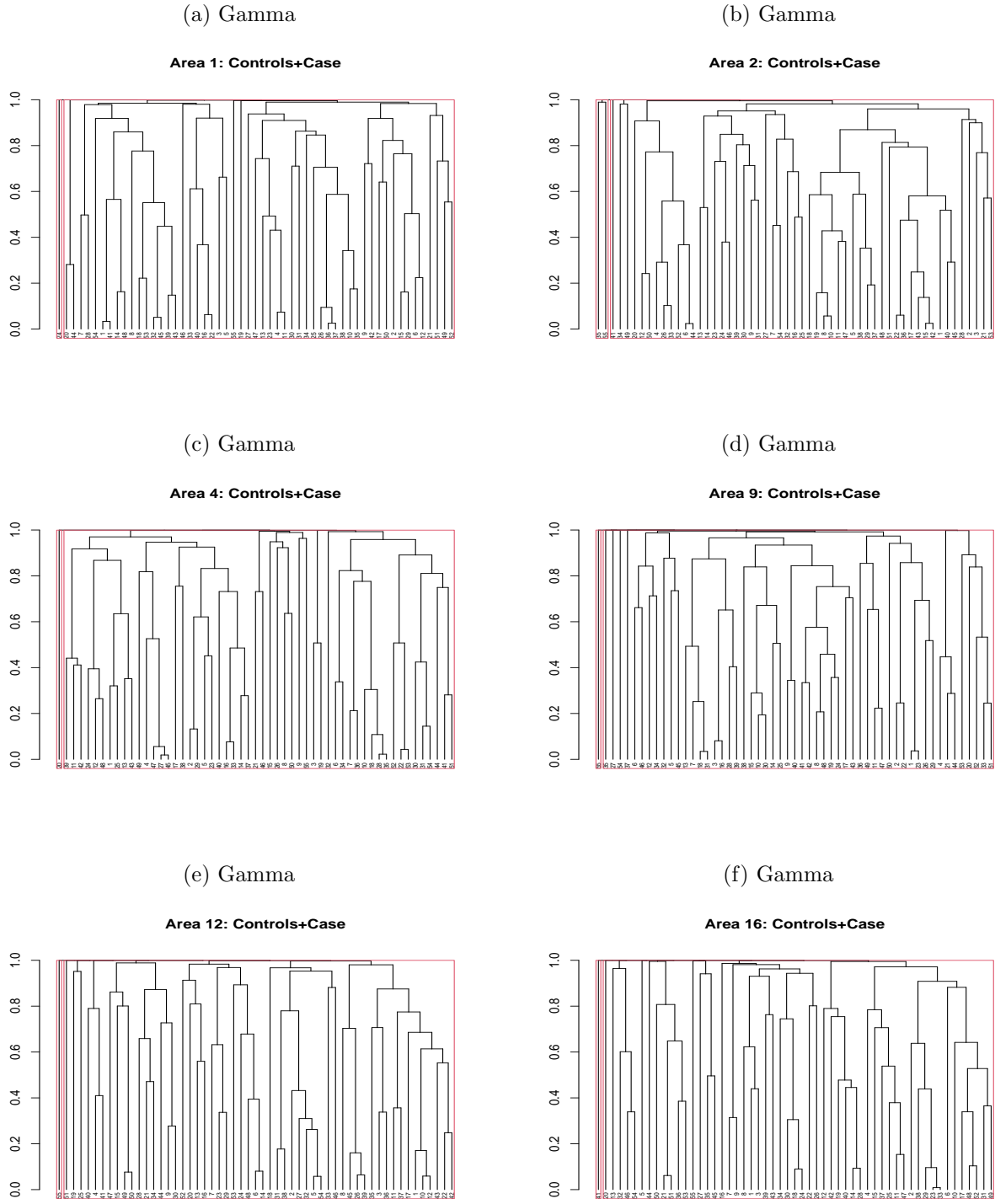


Figure 14: PAD-HC dendrograms in the gamma band. Red boxes indicate the cluster borders if we partition 55 subjects into two clusters.

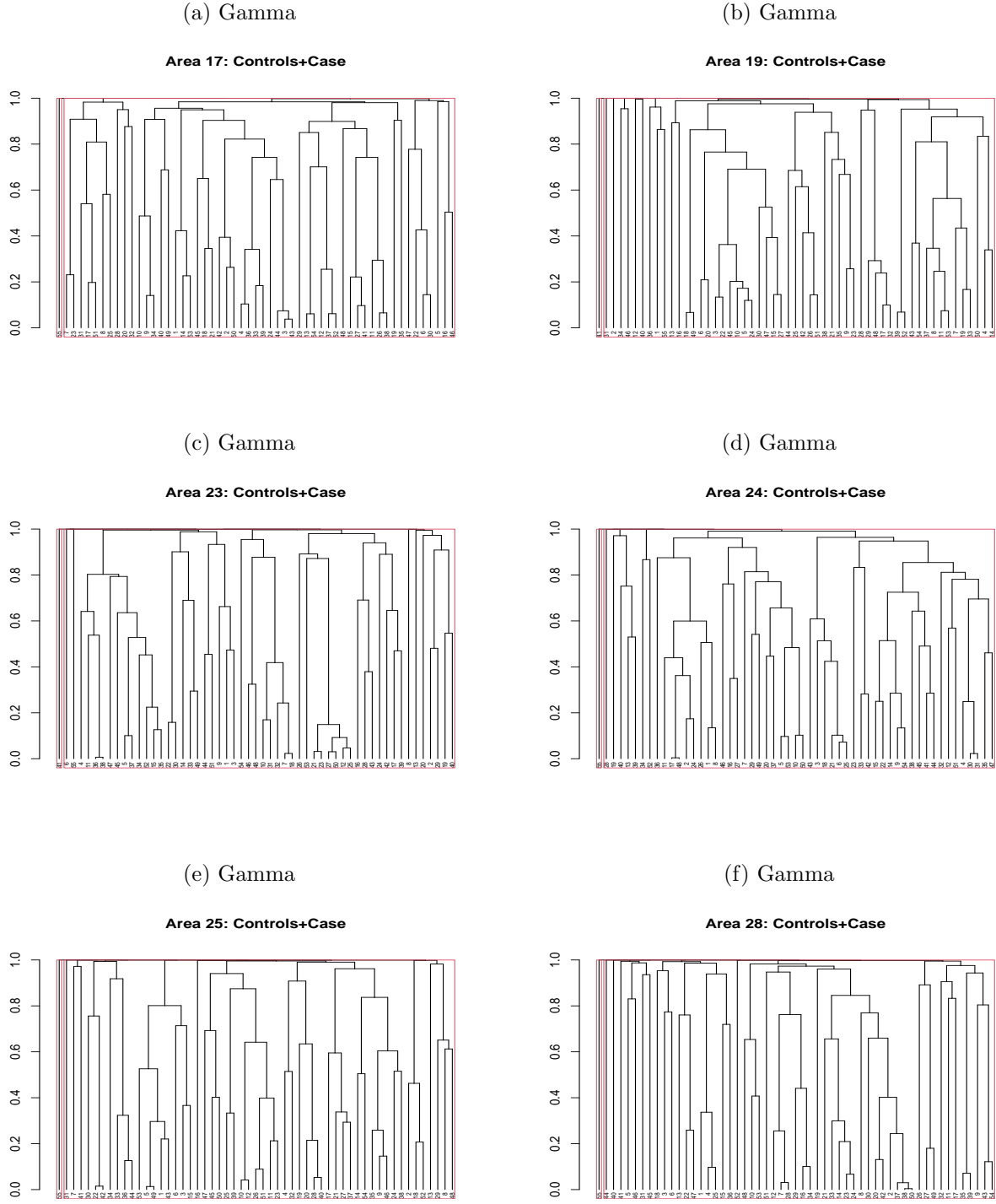


Figure 15: PAD-HC dendrograms in the gamma band. Red boxes indicate the cluster borders if we partition 55 subjects into two clusters.

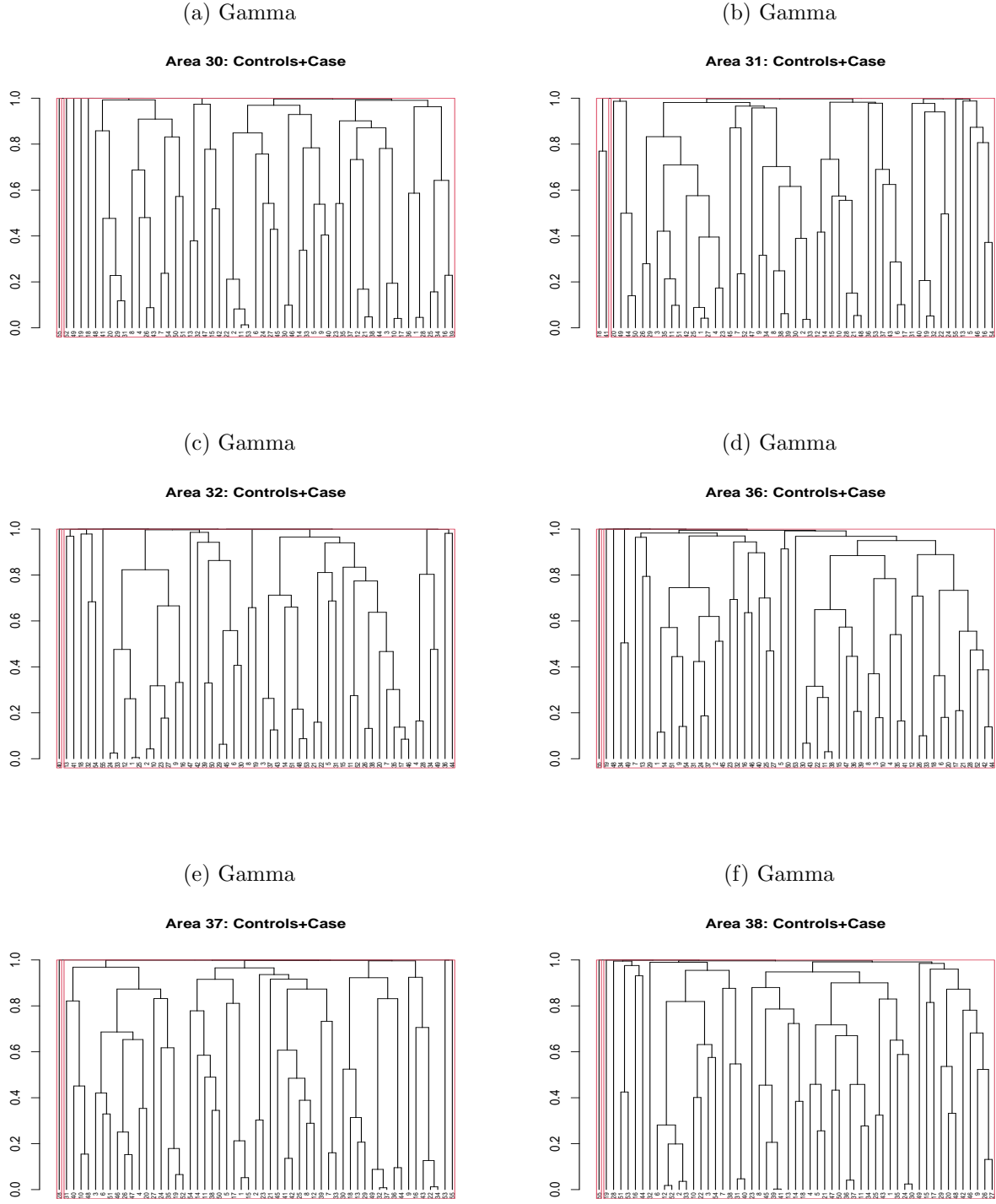


Figure 16: PAD-HC dendrograms in the gamma band. Red boxes indicate the cluster borders if we partition 55 subjects into two clusters.

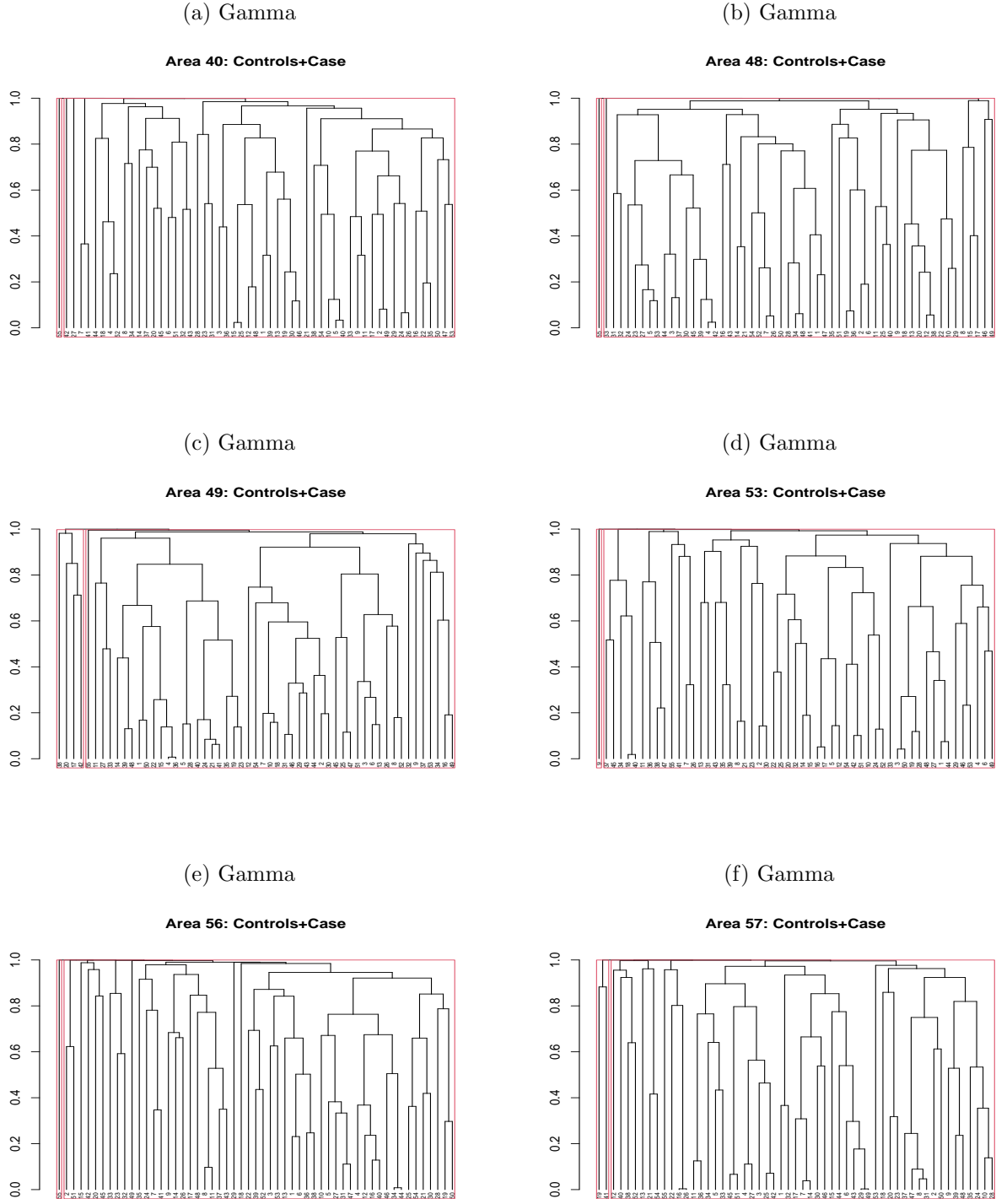


Figure 17: PAD-HC dendrograms in the gamma band. Red boxes indicate the cluster borders if we partition 55 subjects into two clusters.

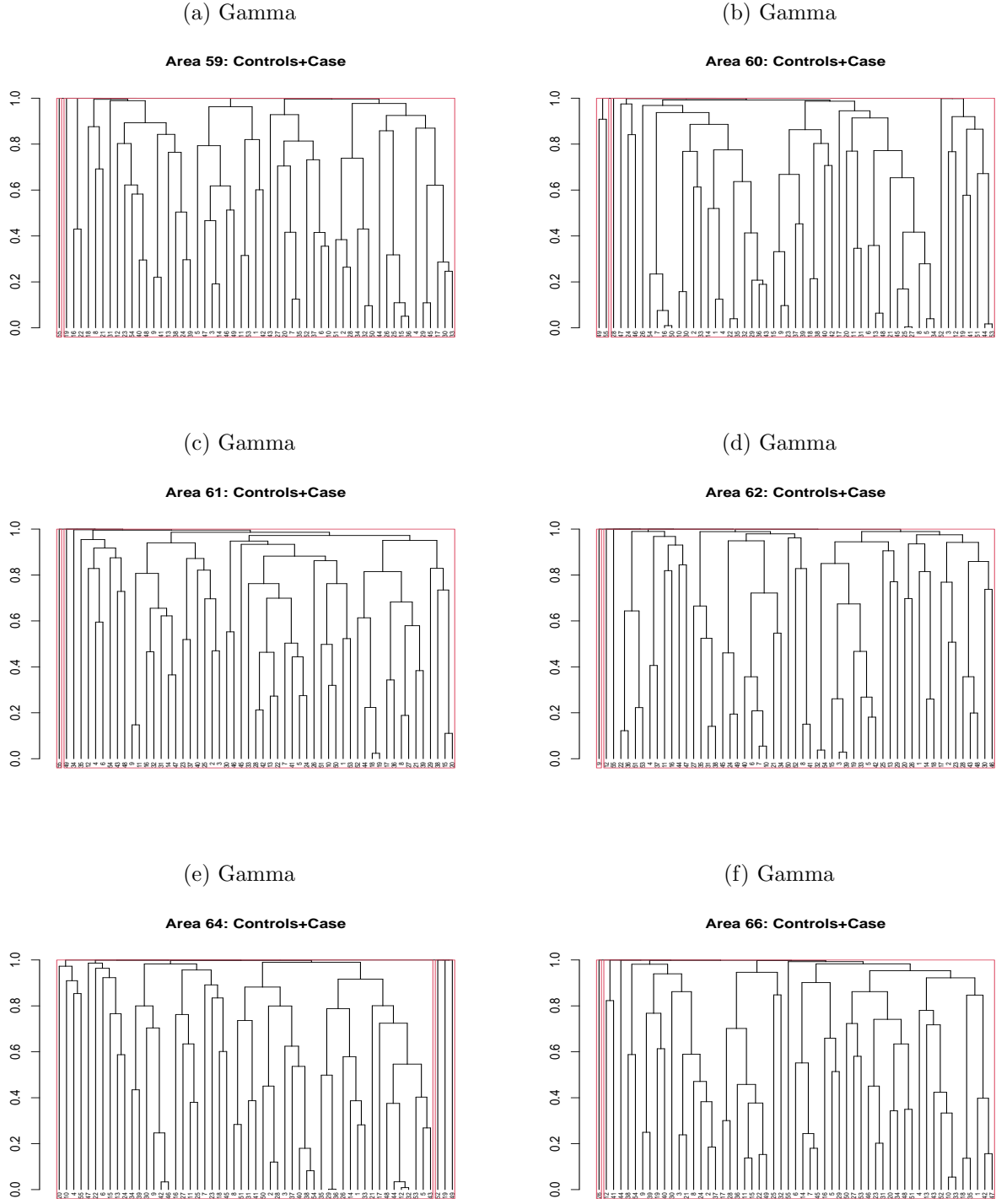


Figure 18: PAD-HC dendrograms in the gamma band. Red boxes indicate the cluster borders if we partition 55 subjects into two clusters.

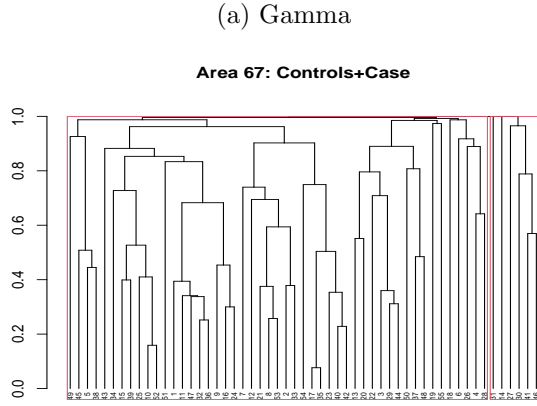
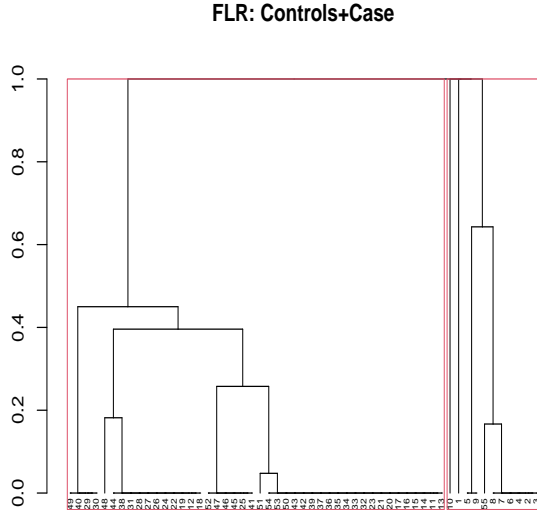


Figure 19: PAD-HC dendrograms in the gamma band. Red boxes indicate the cluster borders if we partition 55 subjects into two clusters.

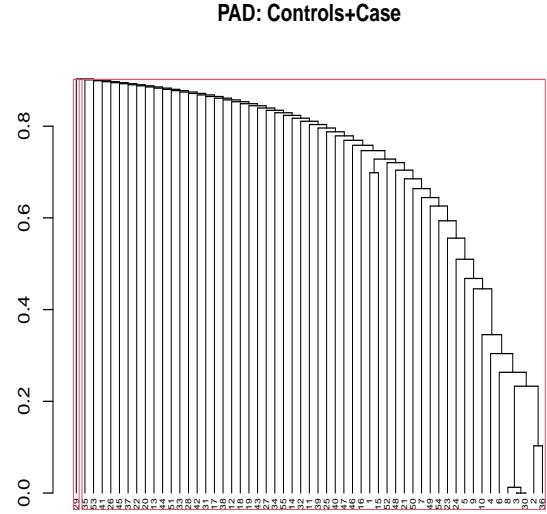
3 Comparison of PAD-HC and FLR-HC

In this section, we demonstrate the abilities of the PAD-HC and the FLR-HC in separating the case from heterogeneous controls by using simulated Settings 1.1, 1.2 and 1.3, where there are two subgroups in controls. It is clearly shown that the FLR is more capable than the PAD to capture heterogeneity in controls and thus to distinguish the case from the controls.

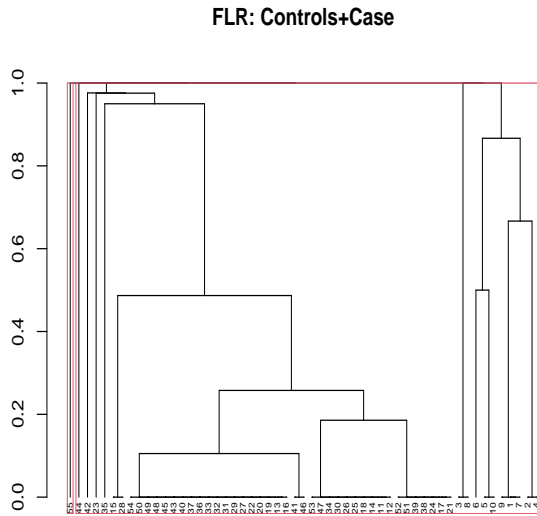
(a) Setting 1.1



(b) Setting 1.1



(c) Setting 1.3



(d) Setting 1.3

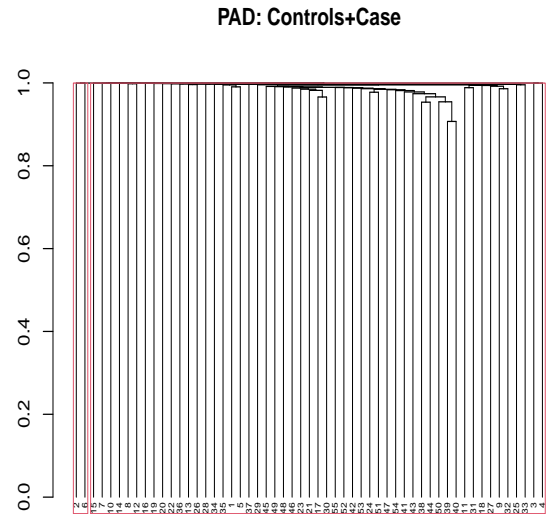


Figure 20: Examples of the FLR-HC dendrograms for the simulated Settings 1.1 and 1.3. Red boxes indicate the cluster borders if we partition 55 subjects into two clusters.

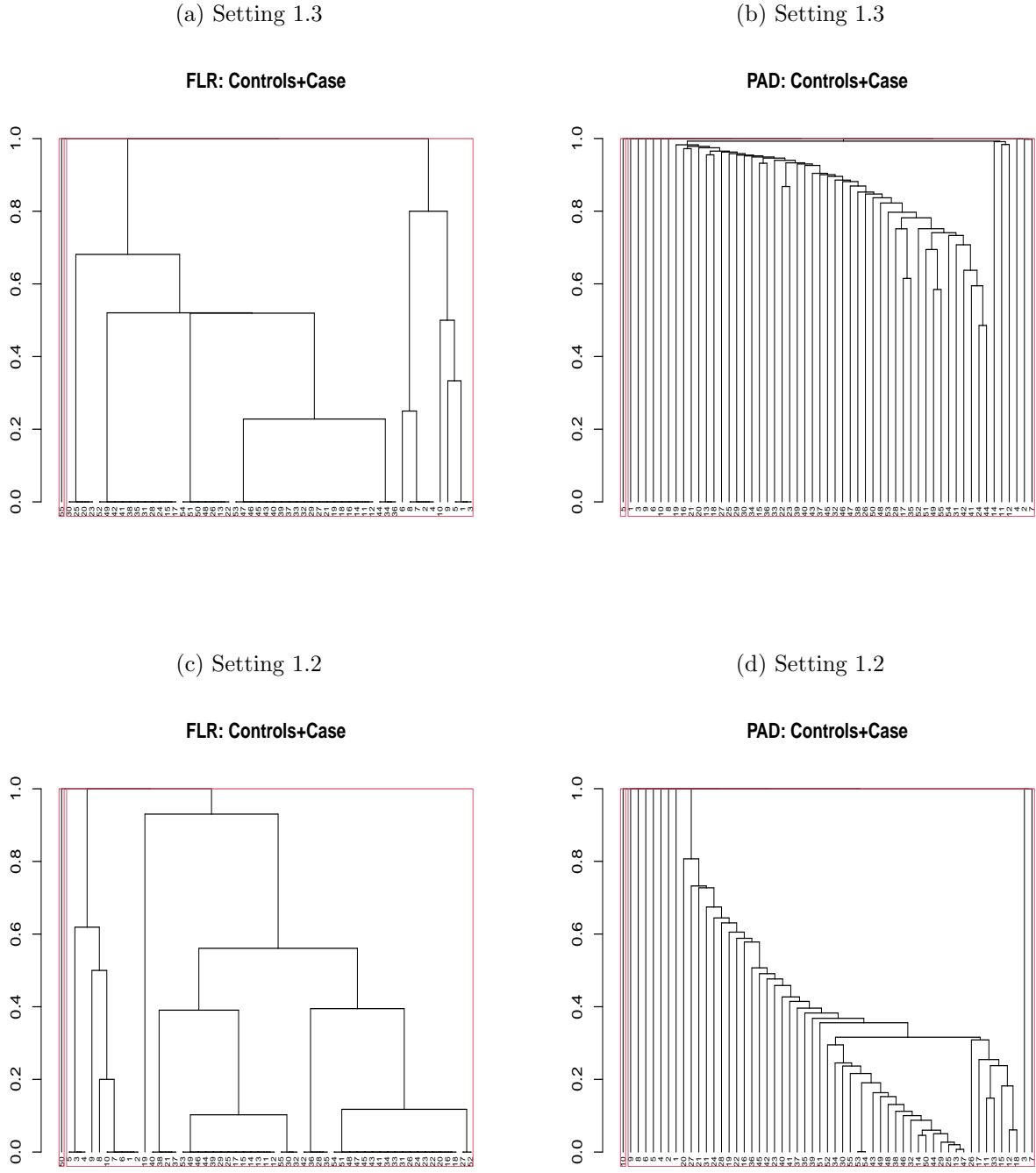


Figure 21: Examples of the FLR-HC dendrograms for the simulated Settings 1.2 and 1.3. Red boxes indicate the cluster borders if we partition 55 subjects into two clusters.